ChemComm

$NaCrO_2$@C Flexible Free-standing Cathode via Electrospinning Technique for Sodium Ion Batteries

Journal:	*ChemComm*
Manuscript ID	CC-COM-05-2023-002610.R1
Article Type:	Communication

COMMUNICATION

$NaCrO_2$@C Free-standing Cathode via Electrospinning for Sodium-Ion Batteries

Received 00th January 20xx,
Accepted 00th January 20xx

DOI: 10.1039/x0xx00000x

Yuanqi Yang,[a] Jinji Liang,[a] Wenya Li,[a] Min liang,[a] Huizi Li,[a] Chenhan Lin,[a] Xi Ke,[a] Zhicong Shi [a] and Liying Liu* [a]

A flexible free-standing cathode is innovatively constructed with $NaCrO_2$ as the electrochemical active substance via an electrospinning technique. As constructed $NaCrO_2$@C flexible free-standing cathode exhibits exceptional rate performance (106 mAh g^{-1} at 10C) and cyclability (retention rate of 87.5% after 300 cycles at 0.2C). This work provides a brand-new perspective to the development of flexible free-standing cathodes.

Flexible electronic products such as roll-up screens, and wearable technology are burgeoning at a surprising pace.[1] Flexible storage systems, as the kernel component of flexible electronics, have attracted extensive attention. Although flexible lithium-ion batteries (F-LIBs) have been commercialized, their sustainable development is being hampered by the limited storage and soaring prices of lithium reserves.[2] Therefore, flexible sodium-ion batteries (F-SIBs) have been considered as one of the most potential alternatives, owning to their abundant resources of sodium and the similar working principles to LIBs.[3] However, F-SIBs are still in their infancy, whose energy density is far below the demands in various application scenarios. Relative to flexible anodes, flexible cathodes for F-SIBs with both excellent electrochemical and mechanical properties are facing particularly huge challenges.

Flexible free-standing cathode is usually composed of active substances and flexible substrates, in which active substances serve as the sodium storaging system. Among the polyanions, layered oxides, and Prussian blue analogues active substances for SIBs, only the polyanionic cathode materials have received more extensive attention such as $NaFePO_4$,[4] $Na_3V_2(PO_4)_3$,[5] $Na_3(VO)_2(PO_4)_2F$ [6] for F-SIBs until now. Generally, flexible polyanionic cathodes are constructed by an electrospinning technique. The electrospinning membrane can be used directly as cathodes without the addition of binders, conductive carbon and collector fluids. And the electrospinning technique offers continuous expressways for electron to improve the electronic conductivity. While the improvement of energy density of flexible polyanionic cathodes is primarily restricted by the limited theoretical specific capacity and large relative molecular mass of polyanionic active substances.[7, 8]

Instead, layered transition metal oxide active substances possess advantages of high theoretical capacity, fast ion diffusion, and high energy density, et al.[9] Flexible free-standing cathodes with transition metal oxides as active substances are usually fabricated via solvothermal synthesis, hydrothermal reaction, and vacuum filtration technique.[10-12] Noting that the success of solvothermal and hydrothermal synthesises depends strongly on the selected flexible substrates which also lower the energy density of flexible cathodes. And the vacuum filtration technique easily causes cathode fracture and stripped active substances during cycling due to the weak adhering interaction between the active substances and flexible substrates. In contrast, cathodes fabricated via the electrospinning are intrinsically flexible without additional flexible substrates and possess strong cohesion between the active substances and flexible substrates. However, oxide active substances are typically synthesized in oxidizing atmospheres which are incompatible with that of electrospinning technology. According to our previous studies,[13,14] layered oxide $NaCrO_2$(NCO) is synthesized in an inert/reducing atmosphere compatible well with that of electrospinning technology, and exhibits superior rate and cyclic performance as well as larger theoretical specific capacity (250 mAh g^{-1}) suitable as the electrochemical active substances for F-SIBs.

Herein, we innovatively proposed to construct a $NaCrO_2$@C(NCO@C) flexible free-standing cathode via an electrospinning technique. The as-constructed NCO@C flexible free-standing cathode exhibits superior rate performance (106.3 mAh g^{-1} at 10C), good cyclability (capacity retention of 87.5% over 300 cycles at 0.2C), and outstanding mechanical flexibility. The current work opens a new avenue towards the future development of flexible free-standing cathodes for SIBs.

According to the PDF Card No. 88–0720, the main diffraction peaks in Fig. 1 can be accurately indexed to the hexagonal layered structure of NCO with a space group *R*-3*m* (166). Noting that, two impurity phases, Cr_2O_3 and Na_2CO_3, are also included with 29 wt% and 14 wt%, respectively. It is reported that Cr_2O_3

[a]. *School of Materials and Energy, Guangzhou Key Laboratory of Low-Dimensional Materials and Energy Storage Devices, Guangdong University of Technology, Guangzhou, 510006, China. E-mail: liyingliusy@gdut.edu.cn (Liying Liu).*
† Footnotes relating to the title and/or authors should appear here.
Electronic Supplementary Information (ESI) available: [details of any supplementary information available should be included here]. See DOI: 10.1039/x0xx00000x

layer coated on NCO can avoid direct contact between NCO and the electrolyte, effectively limiting the incidence of side reactions.[15] The Na_2CO_3 impurity may be resulted from the residual base on the membrane surface reacting with the CO_2 in air. No diffraction peaks of carbon fibre in Fig. 1 reveal that carbon substrate is amorphous.

SEM images of NCO@C free-standing cathode in Fig. 2a shows the consecutive and interlaced fibres with diameters ranging from 100 to 200 nm. The NCO particles about 50 nm are uniformly adhered to or embedded in the interlinked carbon fibres, which are not easily detached during cycling, beneficial for cyclic stability. The elemental mappings captured by EDS (Fig. 2b) demonstrate that the Na, Cr, O, C, and N elements are homogeneously distributed in NCO@C fibres. Meanwhile, Fig. 3a further verifies the presence of Na, Cr, O, C and N elements. In Fig. 3b, four characteristic peaks of C 1s at 284.5 eV, 285.6 eV, 287.9 eV, and 289.5 eV are attributed to C=C, C=N, C-N, and O=C-O, respectively.[16-18] There are three fitted N 1s peaks at 398.3 eV, 400.1 eV, and 403.0 eV assigned to pyridine nitrogen, pyrrole nitrogen and graphite nitrogen, respectively.[19] Notably, the various nitrogen derivated from the PAN precursor can provide more electrons to the π-conjugated system of carbon,[20] thus significantly improve the electronic conductivity of NCO@C flexible free-standing cathode.

As the Fig. S2 shows, the two broad peaks located around 1350 cm^{-1} and 1600 cm^{-1} represent the D-band (related to sp^3 coordination behavior) and the G-band (related to graphite carbon and sp^2 coordination behavior), respectively.[18] The value of R closes to 1.14, indicating good conductivity of carbon framework of the NCO@C flexible free-standing cathode, which is beneficial for improving the electrochemical performance.

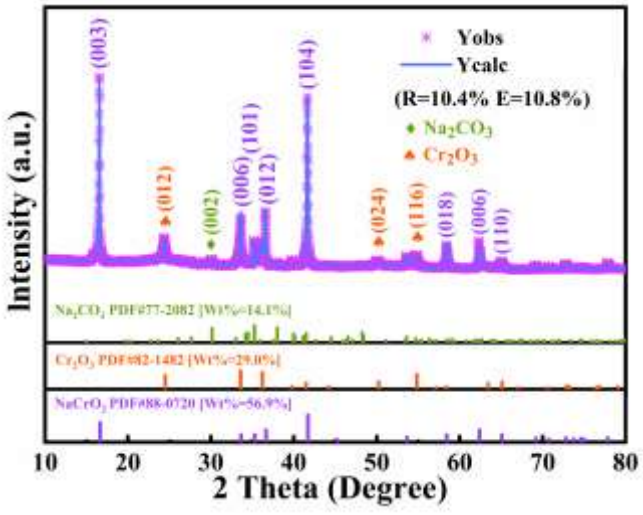

Fig. 1 Refined XRD of NCO@C flexible free-standing cathode.

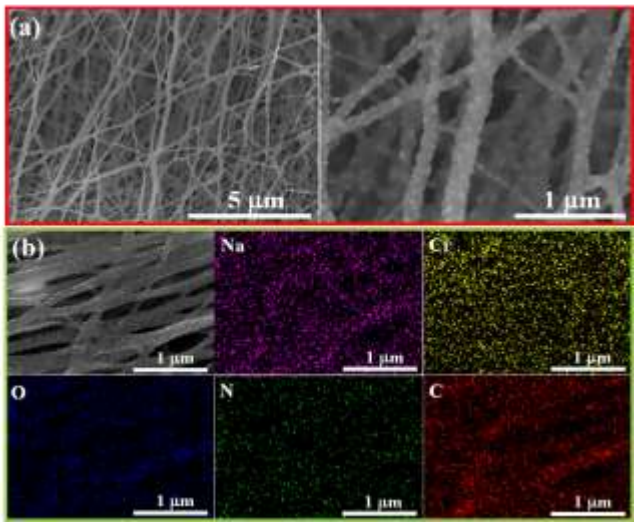

Fig. 2 (a) SEM and (b) EDS of NCO@C flexible free-standing cathode.

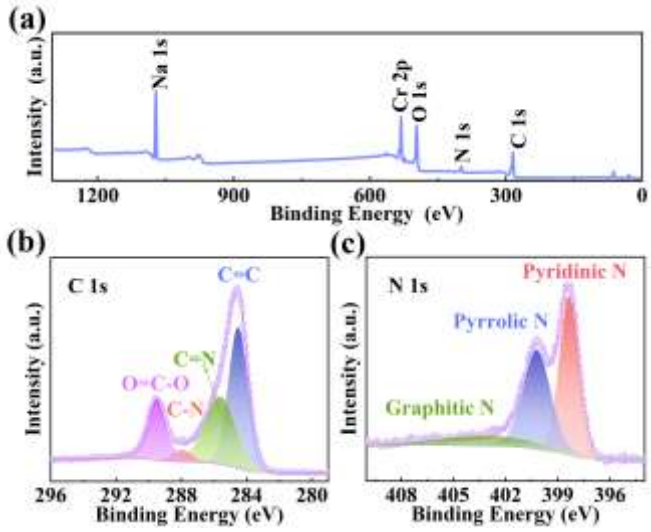

Fig. 3 XPS of NCO@C flexible free-standing cathode: (a) full spectrum, (b) C 1s and (c) N 1s.

Based on the thermos-gravimetric analysis in Fig. S3, the content of NCO substance including Na_2CO_3 and Cr_2O_3 impurities in NCO@C flexible free-standing cathode is 63 wt%. Combined to the refined XRD result (Fig. 1), therefore the calculated content of NCO electrochemical active substance in flexible cathode is 35.8 wt%. In Fig. 4a, the feature of CV curves are well consistent with that of NCO cathode.[21] At 0.1 mV s^{-1}, two pairs of main redox peaks at 3.09/2.83 V and 3.33/3.27 V, correspond to the redox reaction of Cr^{3+}/ Cr^{4+}.[22] And yet the other small peaks in range of 2.9–3.1 V are attributed to the order/disorder phase transformation.[23] The discharge curves in Fig. 4b demonstrate long plateaus at ~3.0 V (vs Na/Na^+) and small plateaus at ~3.3 V, in accordance with two main redox peaks in CV curves. No obvious working potential drop occurs during the initial 20 cycles, indicating the good electrochemical reversibility. The initial discharge capacity of 110.0 mAh g^{-1} is achieved at 0.5C (1C = 250 mA g^{-1}) which is slightly lower than that of NCO cathode in Ref. 18. As shown in Fig. 4c, the NCO@C free-standing cathode delivers an outstanding rate

performance with average reversible capacities of 112.3 112.2, 110.6, and 106.3 mAh g^{-1} at 0.5C, 2C, 5C, and 10C, respectively. When the current density is switched back to 0.5C, the capacity is recovered to 111.2 mAh g^{-1}, very close to the initial value. The initial coulombic efficiency (ICE) in Fig. 4d is 86.2% and the discharge capacity remains at 82.9 mAh g^{-1} after 300 cycles at 0.2C, which illustrates outstanding cyclic stability. The excellent rate and cyclic performance of NCO@C free-standing cathode can be probably ascribed to the following two reasons. On the one hand, the NCO particles are refined by the freeze-assisted sol-gel method, exposing more active sites for sodiation/desodiation and shortening the Na^+ diffusion distance. Meanwhile, the electrospinning technique offers a continuous one-dimensional channel for electron transfer to lower Na^+ diffusion resistance, enabling rapid Na^+ diffusion. On the other hand, the unique cathode structure of NCO active particles embedded in carbon fibres can suppress the volume expansion of NCO during the repetitive Na^+ intercalation/deintercalation to stabilize the crystal structure.

The NCO@C flexible free-standing cathode possesses excellent electrolyte wettability compared to the conventional NCO cathode with aluminium foil as a collector, as shown in Fig 5. The contact angle between the liquid (electrolyte) and the solid substrate (electrode) can be defined by the Laplace-Young's equation:[24]

$$cos\theta = \frac{\gamma_{SV} - \gamma_{SL}}{\gamma_{LV}}$$

where γ_{SV}, γ_{SL} and γ_{LV} represent the thermodynamic surface tensions at the solid-gas, solid-liquid and liquid-gas interfaces, respectively (Fig. 5a). The contact angles are close to 0 ° for both two electrodes in Fig. 5b, c, which are resulted from different reasons. For NCO@C flexible free-standing cathode, the electrolyte is completely absorbed and no visible droplets is left on the electrode surface, while in case of the conventional cathode, the electrolyte just spreads on the cathode surface due to the surface roughness (see Fig. 5d). The excellent electrolyte wettability facilitates adequate contact between the electrolyte and the NCO particles, benefitting for the improved electrochemical performance.

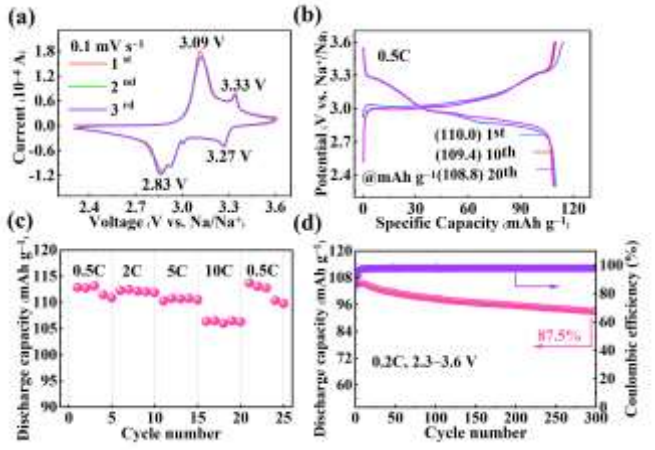

Fig. 4 (a) CV curves, (b) Charge/discharge profiles, (c) rate capability and (d) cyclic performance of NCO@C flexible free-standing cathode. Specific capacity calculated based on 35.8 wt% of NCO in NCO@C flexible free-standing cathode.

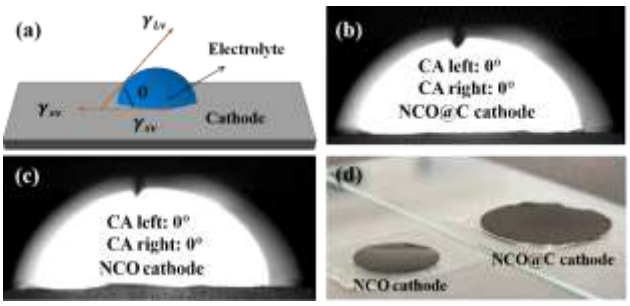

Fig. 5 (a) Schematic representation thermodynamic surface tensions. (b) Contact angle between electrolyte and NCO@C flexible free-standing cathode and (c) conventional NCO cathode. (d) Wettability comparison.

Fig. S4 demonstrates that NCO@C flexible free-standing cathode possesses good bending flexibility. After repeated bending, no fractures or wrinkles occur in NCO@C flexible free-standing cathode when being recovered to its initial state.

The NCO@C flexible free-standing cathode with excellent electrochemical properties and mechanical flexibility was firstly constructed by an electrospinning technique using layered oxide NCO as the electrochemical active substance. The NCO particles are uniformly glued to or embedded in the interconnected carbon fibres, which creates a strong bond between the electrochemical active substance and the flexible substrate. The constructed NCO@C flexible free-standing cathode delivers an impressive rate and cyclic stability performance, with an average discharge capacity of 106 mAh g^{-1} at 10C and retention rate of 87.5% after 300 cycles at 0.2C. The carbonaceous structures constructed by an electrospinning not only contribute to the electron conductivity, but also suppress the volume expansion of NCO during sodiation and desodiation. The combination of oxide-based electrochemical active substances and electrospinning technology sheds a brand-new light on the further development of high-performance F-SIBs.

Conflicts of interest

There are no conflicts to declare.

Acknowledgements

We would like to express our sincere appreciation for the generous financial support provided by the National Science Foundation, China (21673051), and the Natural Science Foundation of Guangdong Province, China (Grant No. 2021A1515010388).

Notes and references

1 L. Zhao and Z. Qu, *J. Energy Chem.*, 2022, **71**, 108–128.
2 N. Tapia Ruiz, A. R. Armstrong and Alptekin, *J. Phys-Energy*, 2021, **3**, 031503.
3 K. Chayambuka, G. Mulder, D. L. Danilov and P. H. L. Notten, *Adv. Energy Mater.*, 2020, **10**, 2001310.
4 Y. Liu, N. Zhang, F. Wang, X. Liu, L. Jiao and L. Z. Fan, *Adv. Funct. Mater.*, 2018, **28**, 1801917.
5 C. Luo, R. Qiu, G. Li, X. Shi, Z. Mao, R. Wang, J. Jin, B. He, Y. Gong and H. Wang, *Mater. Today Energy*, 2022, **30**, 101148.

6 R. Qiu, R. Fei, J. Z. Guo, R. Wang, B. He, Y. Gong, X. L. Wu and H. Wang, *J. Power Sources*, 2020, **466**, 228249.
7 X. Pu, H. Wang, D. Zhao, H. Yang, X. Ai, S. Cao, Z. Chen and Y. Cao, *Small*, 2019, **15**, 1805427.
8 Y. Liu, J. Li, Q. Shen, J. Zhang, P. He, X. Qu and Y. Liu, *eScience*, 2022, **2**, 10–31.
9 Q. Liu, Z. Hu, M. Chen, C. Zou, H. Jin, S. Wang, S. L. Chou and S. X. Dou, *Small*, 2019, **15**, 1805381.
10 L. Xue, X. Shi, B. Lin, Q. Guo, Y. Zhao and H. Xia, *J. Power Sources*, 2020, **457**, 228059.
11 L. Gao, S. Chen, L. Zhang and X. Yang, *J. Power Sources*, 2018, **396**, 379–385.
12 G. Yuan, J. Xiang, H. Jin, Y. Jin, L. Wu, Y. Zhang, A. Mentbayeva and Z. Bakenov, *Electrochim. Acta*, 2018, **259**, 647–654.
13 J. Liang, L. Liu, X. Liu, X. Meng, L. Zeng, J. Liu, J. Li, Z. Shi and Y. Yang, *ACS Appl. Mater. Interfaces*, 2021, **13**, 22635–22645.
14 C. Lin, X. Meng, M. Liang, W. Li, J. Liang, T. Liu, X. Ke, J. Liu, Z. Shi and L. Liu, *J. Mater. Chem. A*, 2023, **11**, 68–76.
15 S. Wang, F. Chen, T. Zhu, X. He, J. Liao, L. Zhang, X. Ding, Q. Hu and C. Chen, *ACS Appl. Mater. Interfaces*, 2020, **12**, 44671–44678.
16 R. Al-Gaashani, A. Najjar, Y. Zakaria, S. Mansour and M. A. Atieh, *Ceramics International*, 2019, **45**, 14439–14448.
17 A. Herath, M. Salehi and S. Jansone-Popova, *Journal of Hazardous Materials*, 2022, **427**, 128167.
18 Q. Ni, Y. Bai, Y. Li, L. Ling, L. Li, G. Chen, Z. Wang, H. Ren, F. Wu and C. Wu, *Small*, 2018, **14**, 1702864.
19 Y. Liu, N. Zhang, L. Jiao and J. Chen, *Adv. Mater.*, 2015, **27**, 6702–6707.
20 X. Zhou, L. J. Wan and Y. G. Guo, *Adv. Mater.*, 2013, **25**, 2152–2157.
21 Y. Wang, W. Li, G. Hu, Z. Peng, Y. Cao, H. Gao, K. Du and J. B. Goodenough, *Chem. Mat.*, 2019, **31**, 5214–5223.
22 L. Liang, X. Sun, D. K. Denis, J. Zhang, L. Hou, Y. Liu and C. Yuan, *ACS Appl. Mater. Interfaces*, 2019, **11**, 4037–4046.
23 S. Wang, F. Chen, H. He, Y. Zhu, H. Liu and C. Chen, *J. Alloy. Compd.*, 2022, **925**, 166690.
24 T. H. Cho, M. Tanaka, H. Onishi, Y. Kondo, T. Nakamura, H. Yamazaki, S. Tanase and T. Sakai, *J. Power Sources*, 2008, **181**, 155–160.